Letters

Reconciling discrepancies in measurements of vulnerability to xylem embolism with the pneumatic method

A comment on Chen *et al.* (2021) 'Quantifying vulnerability to embolism in tropical trees and lianas using five methods: can discrepancies be explained by xylem structural traits?'

Chen *et al.* (2021) reported discrepancies between pneumatic and other methods for measuring embolism vulnerability in plant xylem tissue, leading them to caution against using the pneumatic method. We show that this discrepancy arises from faulty implementation: failing to measure air discharge to sufficiently negative water potentials, they under-estimated maximum air discharge (AD_{max}), and hence embolism resistance. Embolism vulnerability methods identify how dehydrated a stem must become (in water potential, P_{50}) to cause a 50% loss in xylem conductivity. Pneumatic methods require measurements to water potentials roughly twice as dehydrated as P_{50}. Yet Chen *et al.* often stopped at magnitudes even less than what other methods showed P_{50} to be, making it mathematically impossible for their pneumatic implementation to measure true P_{50}. Our simulations confirmed that premature stopping causes large errors in derived P_{50}, accounting for reported discrepancies. Further, literature studies show consistent agreement between pneumatic and other methods. Thus, Chen *et al.*'s pneumatic results are invalid, and should not be taken to undermine confidence in pneumatic measurements. We recommend best practices, including the 'Pneumatron' for automated measurements, that prevent the errors of Chen *et al.* and make pneumatic measurements of embolism vulnerability that are fast, replicable, and accurate.

Introduction

Drought-induced xylem embolism is a potentially important mechanism of plant mortality during a severe drought in natural and agricultural systems (McDowell *et al.*, 2008; Brodersen & McElrone, 2013; Choat *et al.*, 2018), with debate on whether embolisms are a primary causal mechanism, or an associated side effect, of tree mortality (Körner, 2019). This has stimulated research efforts to measure and understand the vulnerability of plants to xylem embolism, which depend on methods for consistent and accurate measurement of xylem traits related to hydraulic failure of the transport system. The parameters measured are often quantified as P_{50} (or P_{88}), the water potential at which plants lose 50% (or 88%) of xylem hydraulic conductivity during a dehydration process (Sperry *et al.*, 2002; Meinzer *et al.*, 2009).

In a recent paper entitled 'Quantifying vulnerability to embolism in tropical trees and lianas using five methods: can discrepancies be explained by xylem structural traits?', Chen *et al.* (2021) (hereinafter simply Chen *et al.*) compared five methods to estimate xylem vulnerability to embolism in terms of P_{50}. Chen *et al.* reported large discrepancies in vulnerability curves obtained with the recently-developed rapid pneumatic method (Pereira *et al.*, 2016) in comparison with the bench-top dehydration method (Sperry & Tyree, 1988), the optical method (Brodribb *et al.*, 2017) and X-ray-computed microtomography (microCT; Cochard *et al.*, 2015). They argue that the pneumatic method, which quantifies the relative increasing volume of air discharged from embolized regions of a branch's xylem (relative to a maximum amount of air discharged, AD_{max}) as the branch is dehydrated in the laboratory, underestimates P_{50} and therefore xylem embolism resistance. Comparisons among methods are important for advancing science, but must be done carefully as there can be important differences in methodological assumptions and practices that create apparent differences in results, which are actually artefacts (Pereira *et al.*, 2016, 2020a,b, 2021; Zhang *et al.*, 2018; Jansen *et al.*, 2020; Sergent *et al.*, 2020).

Here, we show that Chen *et al.*'s reported discrepancy in P_{50} results obtained from the pneumatic vs other methods is an outlier among all studies that have used it; we offer evidence that this anomalous result is likely an artefact caused by inadequate implementation of the pneumatic method by Chen *et al.* in comparison with others who applied this method. Since the pneumatic method is otherwise generally consistent with other methods, we conclude that it in fact offers an effective and reliable way to estimate P_{50} across angiosperm species.

The key problem with the Chen *et al.* implementation of the pneumatic method is evident from their own data, which suggests that a cause of their reported discrepancy is incorrect determination of the maximum air discharge (AD_{max}), a key step in the pneumatic method. Chen *et al.*'s fig. 1(d) (reproduced here as Fig. 1) shows that they did not measure air discharge (blue points and line in Fig. 1) to sufficiently negative water potentials to achieve an accurate estimate of the maximum air discharge. AD_{max}, the maximum amount of air discharged from a branch at the end of a sequence of pneumatic method measurements, is approached when water potential values decline to levels corresponding to 100% loss of branch xylem conductivity. Correct estimation of a true maximum for AD_{max} is necessary to accurately normalize percent air discharge (PAD), the vertical axis of the graph in Fig. 1. Good practice is thus normally to continue measurements until evidence supports a conclusion that

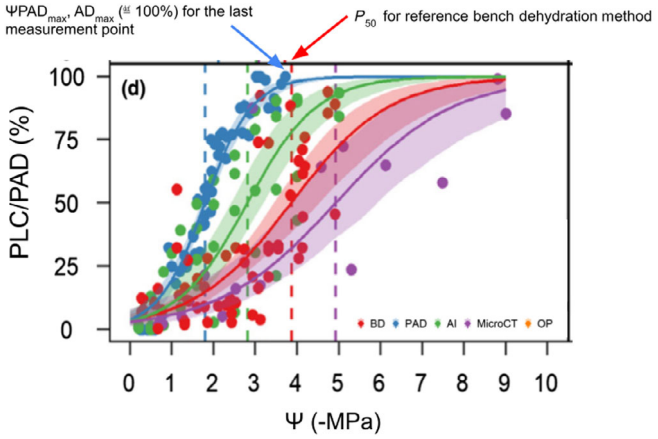

Fig. 1 Reproduction of fig. 1(d) from Chen *et al*. (2021) that shows for the pneumatic method (PAD, percentage of air discharge), xylem water potentials were only taken to a maximum magnitude ΨPAD$_{max}$ (used to estimate the maximum air discharge volume, AD$_{max}$, blue points at 100% PAD on the vertical axis) of *c*. −3.8 MPa, less than half the maximum magnitude of −9 MPa (upper right-hand red point) used for the reference bench-top dehydration (BD) method (red symbols and curves). The water potential value of ΨPAD$_{max}$ is even less than the reference BD method P_{50} value of *c*. −3.9 MPa (vertical dashed red line). This means that if the reference BD estimate for P_{50} was correct, it would be impossible for the implementation of the PAD method shown here to give a correct P_{50}. The shaded areas represent 95% confidence intervals. The other methods are represented as AL, air injection; microCT, microCT imaging; OP, optical method.

AD$_{max}$ has in fact been reached (Pereira *et al*., 2016; Trabi *et al*., 2021). If AD$_{max}$ estimates are too low, the derived percent loss of air discharge (PAD = AD/AD$_{max}$) will be consistently too high, the 50% loss point will be reached too soon, at water potential magnitudes that are too small (i.e. insufficiently negative), and P_{50} will be consistently underestimated. Chen *et al*.'s data (Fig. 1) show precisely this; indeed, their estimates of AD$_{max}$ were in some cases likely to be extreme underestimates, as they were taken at water potentials that did not even reach values as large as the P_{50} value that they were seeking to quantify. Since the P_{50} derived by the pneumatic method should be less negative than the water potential at AD$_{max}$, the pneumatic P_{50} estimated in the example represented by the blue dashed line in Fig. 1 is forced to be substantially less negative than the dehydration method P_{50} represented by the dashed red line. Chen *et al*.'s own analysis thus demonstrates that it would not be mathematically possible for their implementation to give an accurate pneumatically-derived P_{50} estimate, regardless of the branch water status in the branches being measured and regardless of other details or issues that may be associated with the method.

We will offer two independent lines of evidence that support the inference (from Fig. 1) that Chen *et al*. underestimate pneumatic P_{50}. First, we conduct a simulation based on a new dataset that demonstrates the P_{50} artefact caused by a variation in AD$_{max}$ and quantifies its magnitude. We use this simulation to show that the discrepancies reported by Chen *et al*. could arise from stopping the dehydration experiment too soon (as with the blue curve in Fig. 1). Second, we present an analysis, compiled from other recent studies and from our own measurements, that compares the deviation of the P_{50} derived from the pneumatic method to values derived from other methods, showing that Chen *et al*.'s data are anomalous relative to others in the literature.

Materials and Methods

Datasets

We compiled P_{50} and P_{88} data from seven published or in-review studies (Supporting Information Table S1). We added to these datasets new vulnerability curves that we measured on eight tree species from seasonal Amazon forests in Brazil, using both the pneumatic and hydraulic methods as described in Table S2 and Fig. S1.

Data analysis

We conducted two kinds of analyses: first, we conducted simulations based on our Amazon tree species dataset to test the sensitivity of pneumatically derived measurements (P_{50}, P_{88}) to variation in AD$_{max}$; and second, we compared P_{50} and P_{88} measurements derived from the pneumatic method to values derived from other methods across multiple different studies. All data analyses were performed in R software (v.3.5.1; R Core Team, 2020).

Simulating the sensitivity of embolism vulnerability measurements to lower maximum air discharge (AD$_{max}$) in Amazon tree species We used data from eight tree species from a seasonal Amazon Forest (Table S2; Fig. S1) and started with AD$_{max.ref}$, ΨPAD$_{max.ref}$ and $P_{50.ref}$ as reference values, corresponding to our 'best' estimates for the maximum air discharge, and associated maximum water potential and P_{50}, for each species (according to the methods presented in the supplement). We then performed a sensitivity analysis to quantify how sensitive estimates of P_{50} were to artificially reduced values of AD$_{max}$ and ΨPAD$_{max}$ that were at lower magnitudes than AD$_{max.ref}$ and ΨPAD$_{max.ref}$ (taken for the purposes of this simulation as the 'true' values). We simulated several curves for each species, repeatedly recomputing PAD and vulnerability curve parameters for subsets of the curve with consecutively lower AD$_{max}$ values (and correspondingly less negative xylem water potentials). We retained at least the first three most hydrated points (least negative water potentials) in all simulations to have enough points to fit an S-shaped curve. We included all simulated subsets for which the model fit converged (in some cases, a particular subset did not generate a simulated P_{50}, because the fit did not converge due to a low number of points). We used the derived P_{50} values corresponding to each AD$_{max}$ for each species and then quantified the error of this simulated value relative to the 'best' estimate as the ratio $P_{50.simulated}$: $P_{50.ref}$, giving a ratio less than one for simulations that underestimate $P_{50.ref}$.

Quantifying early stopping of the branch dehydration process in pneumatic experiments As a quantitative index of the likelihood that pneumatic measurements of P_{50} were incorrect because of stopping branch dehydration too early (as shown in Figs 1, S2), we defined 'Relative ΨAD$_{max}$', the ratio of ΨAD$_{max}$ (the water

potential of the AD_{max} value used to scale each vulnerability curve) to $P_{50.ref}$, the water potential of the reference 'best estimate' P_{50}:

$$\text{Relative } \Psi AD_{max} = \frac{\Psi AD_{max}}{P_{50.ref}} \quad \text{Eqn 1}$$

Thus, values of *Relative* ΨAD_{max} lower than 1.0 indicate measurements where quantification of air discharge unambiguously stopped too early, at water potentials less negative than that of the independently determined $P_{50.ref}$. Since P_{50} estimated from a vulnerability curve must by definition be smaller in magnitude than ΨAD_{max} (being the water potential where air discharge is 50% of AD_{max}), it is mathematically impossible for such *Relative* $\Psi AD_{max} < 1$ measurements (including the Chen *et al.* measurement depicted in Fig. 1) to provide an estimate of the true P_{50}.

Relative ΨAD_{max} values greater than but still close to 1.0 are likely suspect (because for a typical estimate using symmetric vulnerability curves, P_{50} may be *c.* 50% of the ΨAD_{max}, see Fig. S2). As *Relative* ΨAD_{max} increases to 1.5 or 2.0 or higher, measurements become 'safer' in the sense that they become less likely to suffer errors due to the underestimation of AD_{max}.

We used the Relative ΨAD_{max} index in our sensitivity analysis, using $P_{50.ref}$ as the reference P_{50} value and calculating a separate (simulated) ΨAD_{max} for each simulated vulnerability curve as the AD_{max} was consecutively lowered. We also used low values of Relative ΨAD_{max} to flag potential undermeasurement of air discharge in studies in the literature (including Chen *et al.*), using the P_{50} determined by a comparison method as $P_{50.ref}$ (typically $P_{50\ hydraulic}$). We either used reported AD_{max} or, when the raw data were not available, we estimated from graphs in each study (see Table S1). Where measurements were made on multiple replicate branches, each replicate produces an estimate of AD_{max} and a corresponding water potential (ΨAD_{max}). In this case, we took a conservative approach, taking the most negative ΨAD_{max} value from among replicates for computing Relative ΨAD_{max} for that branch (since the idea was to quantify how negative was the measurement of water potential, relative to the P_{50} parameter, and the most negative of the replicates indicates this).

Assessing the accuracy of pneumatic embolism vulnerability measurements by comparison with other methods in multiple studies P_{50} values were compared across the compiled studies (Table S1), based on the pneumatic, bench-top dehydration (hydraulic), air injection, optical, flow-centrifuge and microCT methods. Because previous studies show that pneumatic measurements on gymnosperms can be difficult to achieve with the manual pneumatic approach (Pereira *et al.*, 2016; Zhang *et al.*, 2018; Sergent *et al.*, 2020), we removed gymnosperm species from our main analyses and included only angiosperm data. Also, we did not distinguish in our analyses the manual pneumatic method from the new automated pneumatic approach using a Pneumatron device introduced to get more consistent results and to reduce variability in the estimated volume of air discharged (Pereira *et al.*, 2020a).

We quantified the differences between values estimated for each method in two ways. First, we directly estimated the difference between values derived from different methods as the root-mean-squared deviation (RMSD) (Piñeiro *et al.*, 2008):

$$\text{RMSD} = \sqrt{\frac{1}{n-1}\sum^{n}(P_x \text{ pneumatic} - P_x \text{ other method})^2} \quad \text{Eqn 2}$$

where P_x means P_{50} or P_{88}, in MPa. In this analysis, we used the bench dehydration hydraulic method as the reference method for Chen *et al.*, in order to simplify our analysis. This strategy was taken because the bench dehydration hydraulic, X-ray-computed microtomography (microCT) and optical (OP) methods yielded comparable P_{50} values in Chen *et al.*'s results.

Second, we tested the null hypothesis that the regression line between pneumatic P_{50} and P_{50} derived by another method was indistinguishable from the 1 : 1 line (i.e. that the slope of that line was indistinguishable from one and the intercept was indistinguishable from zero), across all studies. We used the standardized major axis (SMA) regression ANCOVA test using the SMART package (v.3.4.8; Warton *et al.*, 2012), with the categorical variable used to distinguish the different datasets from the different studies. We tested for differences in slopes (interaction structure) and elevation (additive structure) in linear relationship between the pneumatic and other methods in each study. Using a type II regression approach (i.e. SMA) minimizes residuals in both pneumatic and other methods without assuming (as in ordinary least squares ANCOVA) that error estimates apply only to the *y*-axis variable (Warton *et al.*, 2006, 2012; Wehr & Saleska, 2017). In particular, we were able to determine whether the relationship between methods is consistent across studies, or whether a specific study (e.g. Chen *et al.*) differed from other studies. For that, we used the SMA model to estimate the confidence intervals (CI) of the modelled slope and elevation. When the CI of the estimated slope and elevation overlapped with one and zero, respectively, the P_{50} and/or P_{88} estimates were indistinguishable among methods (Warton *et al.*, 2006). In addition, we also calculated Cook's distance in order to identify data points that have the largest residuals (outliers) or high leverage in the linear regression models fitted (using ordinary least squares) and might have an extreme influence on the regression estimates given by the pneumatic method and other methods (Cook, 1979).

Results

Sensitivity of embolism vulnerability measurements to maximum air discharge (AD_{max})

The simulations of the sensitivity of pneumatic vulnerability curves (including their parameters P_{50} and P_{88}) to using different values of AD_{max} and ΨPAD_{max} are presented in Fig. 2. When we refitted the embolism vulnerability curves scaled by AD_{max} values that were successively less than the best estimate $AD_{max.ref}$, the correspondingly estimated P_{50} values were systematically lower in magnitude, on average, than the best estimate ($P_{50.ref}$), as seen for each of the nine species (Figs 2, S3). The relationship between the P_{50} error

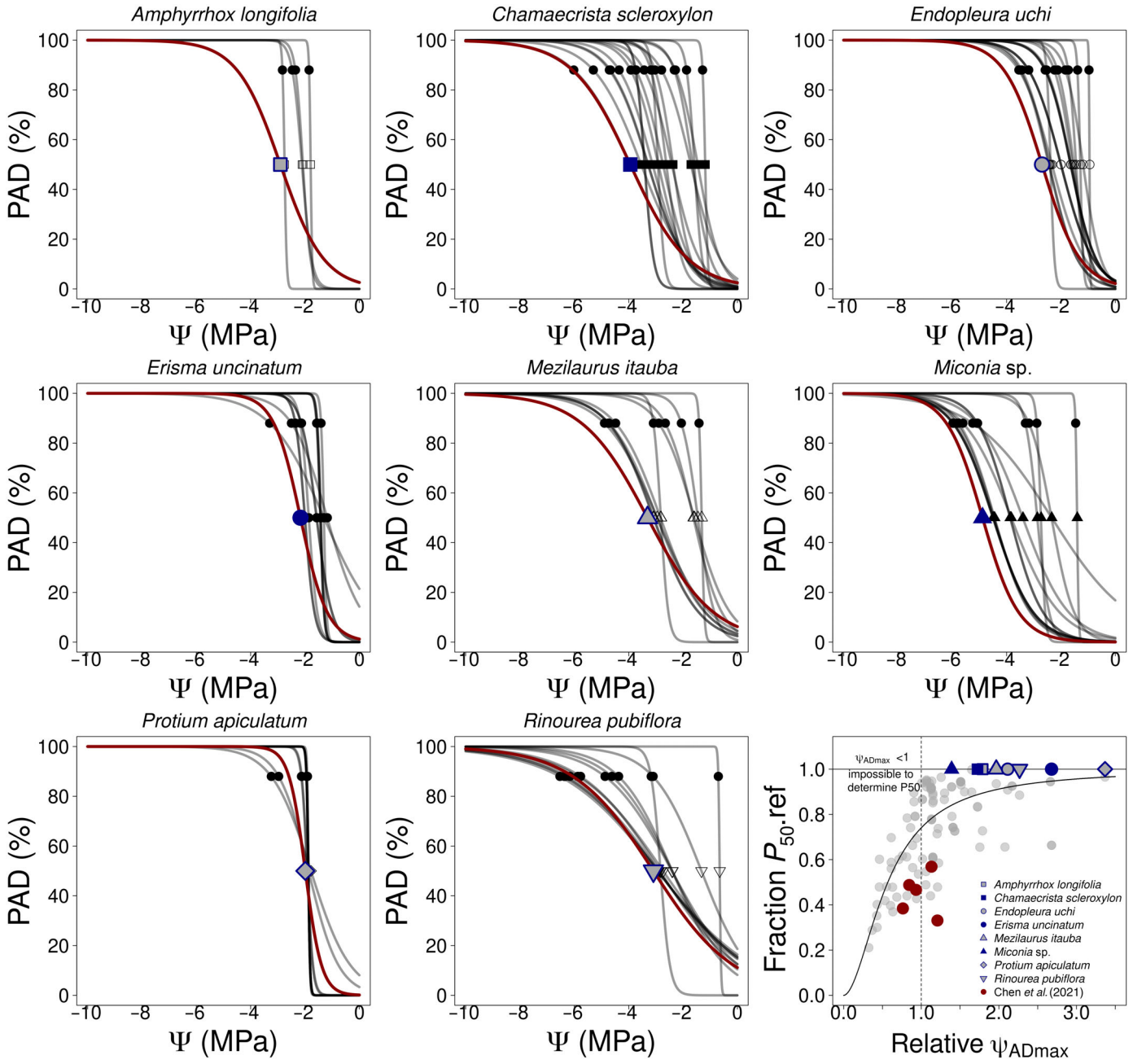

Fig. 2 Sensitivity of pneumatic air discharge (PAD) vulnerability curves (including P_{50} and P_{88} values, the horizontal range of points in each panel, at PAD = 50% and 88%) based on different (artificially reduced) maximum air discharge (AD_{max}) values for tree species in a seasonal Amazon Forest, FLONA-Tapajós, Pará, Brazil. Each grey PAD curve is fitted using a different (progressively lower, relative to the 'true' maximum) AD_{max} value to normalize PAD, hence simulating the effect of incomplete curves, which arise from stopping the dehydration process too early (as we argue was the case in the Chen *et al*. (2021) measurements). The red line represents the 'best' measurement when the maximum air discharge is included. The lower right panel summarizes the simulated error in P_{50} (as a fraction of $P_{50.ref}$, $P_{50.simulated}/P_{50.ref}$, vertical axis) induced by the corresponding simulated underestimates of AD_{max} (horizontal axis) as quantified by the Relative ΨPAD_{max} index (lower values indicate undermeasurement of AD_{max} and its associated water potential), across the eight species and across all simulations. Each grey point corresponds to one simulation and the black line the model fit of $y = x^n/(K_m + x^n)$, where $K_m = 0.34$, and $n = 1.83$. Dark blue and blue outlined symbols represent the 'best estimate' $P_{50.ref}$ for each species listed in the bottom key. The red dots represent the data from Chen *et al*. (2021), with the fractional error (y-axis) computed relative to the hydraulic method ($P_{50\ pneumatic}/P_{50\ hydraulic}$).

(simulated P_{50} as a fraction of the reference $P_{50.ref}$, so that 1.0 = no error, and a value < 1.0 means an underestimate) and the index of premature stopping (Relative $\Psi AD_{max} = \Psi AD_{max}/P_{50.ref}$) across all species (Fig. 2 lower right summary panel) showed that simulated P_{50} was consistently lower than $P_{50.ref}$ when AD_{max} was too low (with Relative $\Psi AD_{max} < 1.0$ indicating extremely low values) and rose towards matching $P_{50.ref}$ (horizontal line at Fraction $P_{50.ref} = 1.0$) as Relative ΨAD_{max} increased. This

relationship is summarized by a fit to the curve $y = x^n/(K_m + x^n)$ (the generalized Michaelis–Menten model, with $K_m = 0.34$, and $n = 1.83$, Obs vs Pred$^2 = 0.47$; $P < 0.001$). The magnitude of the P_{50} discrepancies associated with the underestimation of AD_{max} varied among species (as seen by the scatter in Fig. 2 lower right, broken out in panels of Fig. S2).

We plotted the values of the Chen *et al.* measurements (taking their hydraulic P_{50} as $P_{50.ref}$ for calculating the relative error of their pneumatic P_{50} and the Relative ΨAD_{max}) on the same summary graph as our simulations (red points in Fig. 2 lower right summary panel). We found that most (three of five) of the Chen *et al.* vulnerability curves were based on Relative $\Psi AD_{max} < 1.0$ (indicating impossible-to-estimate P_{50}). The Chen *et al.* values showed slightly more error, on average, than our simulated errors (fraction of $P_{50.ref}$ was lower than the fitted curve in Fig. 2), so some portion of their reported difference between pneumatic and other methods may have been caused by other factors (or by moderate intrinsic differences among methods). However, most Chen *et al.* points fell within the cloud of our simulated points, suggesting that Chen *et al.*'s pneumatic errors are consistent with errors due to premature stopping.

Comparison of the pneumatic method to alternative reference methods

Considering the full datasets of all studies (Table S1), we found broad agreement between pneumatic estimates of P_{50} as compared to estimates derived from other methods (Table S3) – except for the Chen *et al.* study, which stands out as anomalous (Fig. 3a). Chen *et al.* was the only study that did not show consistency between pneumatic P_{50} estimates and those derived from other methods, with a slope far different from 1 (Fig. 3b), the largest disagreement between methods (RMSD = 2.7 MPa) and a greater difference in the intercept, which had the largest error range of the studies (Fig. 3b; Table S3). The other six studies' regression lines agreed with the 1 : 1 line within 95% confidence (except Paligi *et al.* which, though its slope was indistinguishable from 1, had an elevation just slightly statistically > 0 – Table S3), including Sergent *et al.* (2020), which reported apparent discrepancies for long-vessel species (but see Pereira *et al.*, 2021), and presented the second largest RMSD among all studies (1.57 MPa; Fig. 3b). Considering individual points in the studies, one data point from Chen *et al.* and three from Sergent *et al.* (2020) were considered as outliers according to Cook's distance (Fig. S4).

As indicated by the discussion in the Introduction section regarding Fig. 1, the pneumatic measurements reported by Chen *et al.* were mainly taken during early and middle phases of the dehydration process, with none of the primary measurements reaching the late stage of dehydration necessary to obtain complete vulnerability curves and accurate estimates of AD_{max} and hence of P_{50} (though we note that one species was further analysed separately in Chen *et al.* fig. 6, see the Discussion section). In all cases, the xylem water potentials corresponding to AD_{max} determined for the pneumatic method were not even half of the water potentials

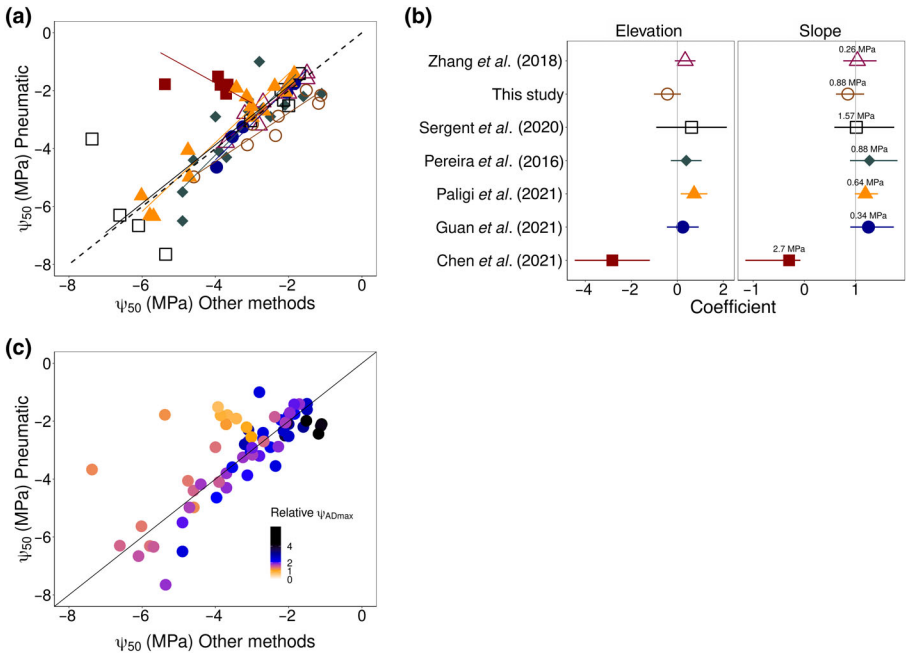

Fig. 3 (a) P_{50} derived from the pneumatic method plotted vs alternative methods. Dashed black lines show the 1 : 1 relationship, and the seven coloured lines represent different datasets as compiled from the indicated publications and treated in an standardized major axis (SMA) ANCOVA as a categorical variable; (b) the elevation (left) and slope (right) and 95% lower and maximum confidence interval (horizontal lines) derived from the SMA ANCOVA test, with the vertical black line representing the 1 : 1 slope and zero intercept. Overlapping 95% confidence intervals test the null hypothesis (slope = 1; elevation = zero) that the pneumatic method is indistinguishable from the other methods (see also Supporting Information Table S3). Values on the right side represent the root-mean-squared deviation (RMSD), which computes the square root of the mean of the squared deviations in P_{50} between the pneumatic method and alternative methods. (c) Reproduction of the graph in (a) showing (in colour code) the value of Relative ΨPAD_{max} (Eqn 2). Here, we show that the one likely reason that the Chen *et al*. (2021) data disagree with other studies is that Relative $\Psi PAD_{max} \lesssim 1$ (see Eqn 1), indicating that they use a reference AD_{max} much before the branch was completely dehydrated. The continuous black line represents the 1 : 1 relationship.

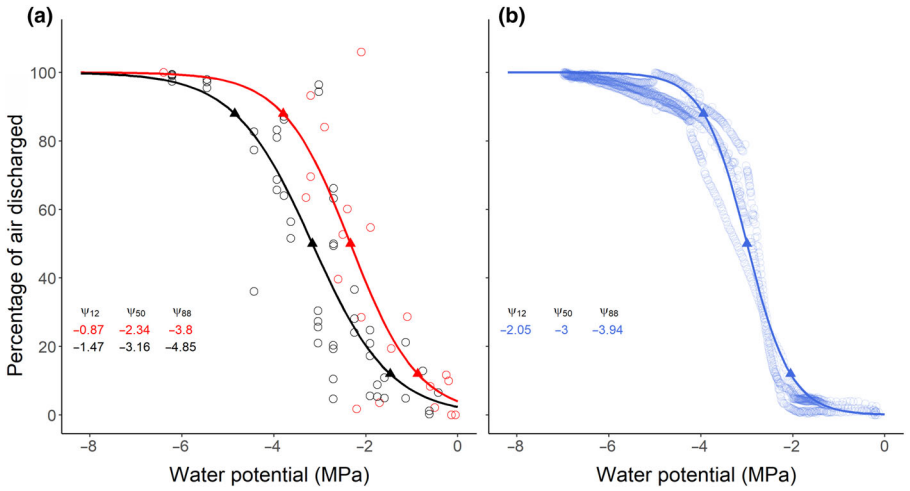

Fig. 4 Comparison of datasets generated by (a) the manual implementation of the pneumatic (in red, as used here and by Chen *et al*., 2021) and hydraulic (in black) methods vs (b) the automated method (in blue, Pneumatron, data from Pereira *et al*., 2016, 2020a) for a *Schinus terebinthifolius* tree (see referred papers to understand methods). The points are observations of air discharged, and the lines are the fitted vulnerability curves based on the logistic function (Pammenter & Vander Willigen, 1998) with the respective P_{12}, P_{50} and P_{88} highlighted (triangles). The Pneumatron measures more frequently and precisely the air discharged and can give a reliable estimate of embolism vulnerability parameters (P_{12}, P_{50} and P_{88}) directly from the data without fitting, and these can be estimated for individual branches (not shown here), whereas the noisiness of the manual approach requires multiple replicates to produce good estimates.

determining the maximum percentage of loss of hydraulic conductivity with the other methods (Fig. 3c colour code), with four out of five measurements stopping at water potential magnitudes of 4.5 MPa or less (and one reaching a magnitude of 6.5 MPa). The lesser Relative ΨAD_{max} (indicative of stopping measurements sooner) the more insufficient was AD_{max}, and the more the pneumatic method underestimated $P_{50,}$ (yellowish colours with Relative ΨAD_{max} lower than 1; Fig. 3c). By contrast, when Chen *et al.* used nonpneumatic methods, they estimated the embolism resistance using the maximum amount of embolized vessels taken at more negative xylem water potentials (frequently more negative than −6.5 MPa).

Discussion

Our primary finding is that the large discrepancy between the pneumatic and other methods reported by Chen *et al.* is inconsistent with previous studies comparing pneumatically derived embolism resistance to other methods in angiosperm species, including six published studies and a new dataset updated from that of Brum *et al.* (2019) (Figs 3, S2). The discrepancies reported by Chen *et al.* are almost certainly due to incorrect implementation of the pneumatic method, namely underestimation of the maximum amount of air discharged from xylem (AD_{max}) due to stopping the measurements before reaching sufficiently negative water potentials. This conclusion is supported here by simulations (Fig. 2) and by the fact that deviations between pneumatic and hydraulic methods occur precisely for measurements with Relative $\Psi PAD_{max} < 1.0$ (indicating AD_{max} taken before sufficient branch dehydration, which pulls those pneumatic data points far away from the 1 : 1 relationship) (Fig. 3c). In many cases, Chen *et al.* halted their pneumatic measurements at potentials so low in magnitude that they fell short of the xylem tissue's putative P_{50}, making it mathematically impossible for their pneumatic estimates to match that putative value (which was obtained by other methods that they implemented in a way that did achieve sufficiently negative water potentials). We conclude that Chen *et al.*'s reported results for the pneumatic method are invalid and should not be used for scientific analysis of embolism vulnerability and, in particular, should not be taken to undermine confidence in pneumatic measurements of embolism resistance.

We note here that a significant recent advance in the application of the pneumatic method (the automated Pneumatron device, Jansen *et al.*, 2020; Pereira *et al.*, 2020a) makes the pneumatic method much easier to use and makes it virtually impossible (even for inexperienced users) to create the kind of implementation error found in Chen *et al.* The Pneumatron generates more data of much greater internal consistency and thus less noise, compared with manual measurements (Fig. 4), and the achievement (or lack) of a saturating level of air discharge is evident from the data directly. The Pneumatron may also allow the pneumatic method to be applied more generally, including to gymnosperms, which previously had given problematic results (it is for this reason we focussed only on angiosperm species within the cited studies) (Sergent *et al.*, 2020; Pereira *et al.*, 2021). For detailed practical advice on the construction and use of the Pneumatron (including open-source software for study, modification and distribution by anyone), and guidance on best practices for implementing high-quality pneumatic measurements generally, we refer readers to Trabi *et al.* (2021).

Chen *et al.* offer a list of potential causes of their reported underestimates of pneumatically derived P_{50}, which they suggest cautions against trusting the pneumatic method generally. Given the analysis presented here, however (that no other study finds the discrepancy reported by Chen *et al.* and that this discrepancy likely arises from inadequate implementation of the methods that render the results invalid artefacts), the evidence suggests caution should rather be applied to the Chen *et al.* measurements. However, as it is generally important to consider all potential sources of error in a

New Phytologist

given measurement, and Chen *et al.* do raise much-discussed issues that we agree are important for users of embolism vulnerability estimates to be aware of, we review them here, drawing on earlier work (Pereira *et al.*, 2016; Guan *et al.*, 2021; Yang *et al.*, 2021) including references to 'best practice' for implementing the pneumatic method.

The concerns listed by Chen *et al.* are: (1) that the pneumatic method may be biased towards measuring the vulnerability of vessels at the cut end of a measured branch and these vessels are supposed to be made more vulnerable by the cutting; (2) that there are systematic uncertainties in estimating the AD_{max}, which Chen *et al.* illustrate with a more detailed analysis on one of their species whose embolism vulnerability curve purportedly exhibits two distinct plateaus during the dehydration process, raising a question as to how investigators can tell when saturation in air discharge has been reached (see fig. 6 in Chen *et al.*); (3) that there are uncertainties regarding the source of air discharged in the pneumatic measurements; and/or (4) that branch vessel shrinkage or cracks may allow gas leaks which undermine pneumatically-derived quantities.

With regard to (1), the potential special susceptibility of the cut end of the branch due to the cutting itself: it is important to clarify a potential confusion here and distinguish cut-open conduits from intact ones. Conduits that have been cut open for the purposes of making the pneumatic measurements quickly become gas-filled and should be considered an extension of the discharge tube. They are effectively not a part of the sample being measured and should not bias the measurement. Indeed, the quantification of the minimum air discharged, AD_{min} (at the beginning of the measurement), accounts for air in the cut-open vessels. The proximity of gas in cut-open conduits may slightly facilitate embolism propagation in the early stages of measurement (a possible explanation for why P_{12} values based on pneumatic measurements can be more vulnerable than embolism spreading in intact samples, Pereira *et al.*, 2016; Paligi *et al.*, 2021). However, the available evidence shows that the detection of xylem vulnerability in the whole branch should not be limited to the cut end, or exacerbated by the cutting beyond the initial stages, because embolism propagates throughout the whole branch from previously embolized vessels (Choat *et al.*, 2016; Hochberg *et al.*, 2016), to others, but this happens only so long as the water potential is low enough to nucleate large bubbles whose propagation is derived from an embolized to an adjacent vessel (which is what the measurement itself induces by design, with increasing dehydration). In the end, the user should, in any case, find confidence in the consistency that is generally seen between the pneumatic and other methods in the literature beyond Chen *et al.* (Fig. 3), which suggests there is not a significant or special vulnerability introduced at the cut end of branches measured with the pneumatic method.

Regarding (2), uncertainties in estimating AD_{max}: these are quite possible when the manual pneumatic method is incorrectly implemented (as illustrated by the problems in the Chen *et al.* dataset), but also, with careful attention to detail, quite avoidable, as illustrated by the other, non-Chen *et al.* studies reviewed here (which have all managed to produce pneumatic method estimates consistent with other methods), and also by the automated Pneumatron, which makes it difficult to underestimate AD_{max} (Fig. 4). Chen *et al.* do conduct a measurement test to greater dehydration on one of their species, arguing that the resultant embolism vulnerability curve exhibits two distinct plateaus in air discharge (thereby introducing ambiguity about what AD_{max} should be) when dehydration is carried out to extreme negative water potentials, which they report reached −20 MPa (see Fig. S5, which reproduces panels from Chen *et al.* fig. 6).

Putting aside the question of the reliability of water potential measurements to extreme values like −20 MPa, Chen *et al*'s fig. 6 (Fig. S5 here) seems to illustrate our point: when they stopped at an early water potential value (blue points and curve in Fig. S5), Chen *et al.* calculated a P_{50} of −1.58 MPa. Including all the points to −20 MPa, and rescaling (red points and curve), they calculate a P_{50} of −6.32, which is right in the middle of the range of values from other methods they reported earlier in the manuscript (from −5.38 for hydraulic to −5.45 for optical to −7.48 for microCT). However, scepticism is warranted: (1) water potentials more negative than −10 MPa are outside the range of the instruments used by Chen *et al.* (ICT electronic psychrometers and pressure bomb), and these stem water potentials were not observed, but extrapolated from a relationship between drying time and water potential (parameters and model were not shown in their paper and raises questions about how such extrapolations, of a nonlinear process, might have been validated); (2) water potentials between −10 and −20 MPa, if real (they are rarely seen in the plant hydraulic literature), would bring branches close to a desiccation-induced destabilization of cell interior lipid bilayers, which limits the tolerable negative pressures in plants to values above −10 MPa, thereby limiting plant functioning (Kanduč *et al.*, 2020). This desiccation point would likely make branches subject to cracking and air leakage through tight-fitting hose clamps from the pneumatic apparatus. Finally, (3) the reported double plateau (Fig. S5) is hard to discern amidst noisy data (Chen *et al.* make no statistical or other objective test of the existence of two plateaus, and we would challenge anyone looking at Fig. S5 to consider whether separate plateaus are clearly evident with respect to the salient variable of water potential, either within individual replicates in panel b, or in the whole dataset of panel c). In any case, the putative second plateau (between −10 and −20 MPa) consists only of extrapolated water potentials, while the first plateau's water potentials are directly observed, raising the question of whether the double plateau, if it exists, might be an artefact of a mismatch between observation and extrapolation. We are sceptical that the second plateau is really useful, or a problem to fit the pneumatic curve, or that would be also a problem for any other method. In any case, we believe that especially with the advent of new approaches (e.g. Pneumatron, Fig. 4b) that automatically continue the measurement until a plateau is reached, the issue of uncertainties in identifying AD_{max} will be minor for future measurements via the pneumatic method.

It is important to keep in mind that the issue of identifying a reliable benchmark for scaling datasets is not unique to the determination of AD_{max} for the pneumatic method, but also applies to other methods, including the optical method, which uses the maximum embolized area based on pixels, an area that is

determined only at the end (Brodribb *et al.*, 2017; Guan *et al.*, 2021). This contrasts with hydraulic conductivity-based measurements of embolism resistance, in which the maximum hydraulic conductivity is obtained in the beginning (assuming PLC = 0%), while AD_{max} can only be obtained at the end of a pneumatic experiment when the slope of AD in response to a decrease in xylem water potential is close to zero. Therefore, methods that rely on hydraulic conductivity have a clear difference in temporal sequence in reaching these two reference points for normalization. Users of the pneumatic method must be careful to have a good starting point (Kh_{max}; AD_{min} in the more hydrated water potential state), as well as a defined endpoint (AD_{max}), which is clear only when a stable plateau of AD_{max} is obtained.

With respect to (3), the source of discharged air: both experimental work and models on gas diffusion kinetics across xylem conduits provide evidence that the pneumatic method measures directly gas that is extracted from embolized, intact conduits due to the fast movement of gas across pit membranes (Jansen *et al.*, 2020; Pereira *et al.*, 2020b; Guan *et al.*, 2021; Paligi *et al.*, 2021; Trabi *et al.*, 2021; Yang *et al.*, 2021; Avila *et al.*, 2022; Peng *et al.*, 2022), while gas diffusion across conduit cell walls is much slower (Sorz & Hietz, 2006; Wang *et al.*, 2015). Although the mass flow of gas is 10 000 times faster than the diffusion of gas through a liquid, the thin nature of pit membranes makes the diffusion of gas across pit membranes still very fast (within seconds) (Yang *et al.*, 2021). There is solid evidence that the gas source is mainly and directly extracted from embolized, intact conduits during the first 15 s (Yang *et al.*, 2021), well supporting the theoretical basis for the pneumatic method. However, there are some cases where leakage may nonetheless be a source of uncertainty in the pneumatic method (see the next point).

With respect to (4), gas leakage due to shrinking or cracks: we agree that cracks or leaky pith tissue can be problematic, especially in nonwoody plants, or when the water potential is more negative than −10 MPa (as in the second plateau of Chen *et al.*, Fig. S5), but we have not seen evidence in our own work with woody plants and measurable water potentials (despite our careful attention to the risk of leaks), and are not aware of evidence from others, that possible cracks are substantially connected to the cut-open conduits and thence to the pneumatic apparatus. However, we think that difficult-to-detect micro-cracks or shrinkage-induced leakage might nonetheless be contributing to the range of uncertainties normally seen in even correctly applied implementations and that these do warrant continued attention as the method develops. For example, shrinkage near the cut-open tissue might cause potential small air leaks through tight-fitting hose clamps (Trabi *et al.*, 2021).

In sum, we agree that there are many nuances to xylem anatomical function under hydraulic stress that are not fully understood and that these nuances likely contribute to the normal range of uncertainty seen in this and all methods that focus on characterizing xylem vulnerability. However, based on pneumatic experiments with many species, we do not think that any of these nuances (aside from the large errors in AD_{max} identification exhibited in Chen *et al.*) raise concerns that undermine the value of pneumatic measurements *per se*, any more than comparable errors in the other methods negate the careful application of those methods. As in all methods, careful application of best practices, in this case including careful checking (or alternatively, use of the Pneumatron apparatus, Fig. 4) to assure that an AD_{max} plateau has been reached, and examination of samples during and after measurement to assess signs of degraded sample quality (presence of visible cracks, resins, etc.) should give users confidence in the results of pneumatic measurements (Trabi *et al.*, 2021).

Beyond these specific issues, an important theoretical question is: why should we expect these diverse methods (pneumatic, hydraulic, microCT observations of embolism and optical) to converge on a common estimate of embolism resistance? Addressing this question requires careful consideration of our mechanistic understanding of the anatomy and biological functioning of xylem tissue in plants, and what exactly is being measured. More work, however, is needed to fully understand gas movement in the xylem (including diffusion and mass flow), which affects the duration of pneumatic experiments, and how gas movement relates to embolism propagation from an embolized to a neighbouring conduit (Jansen *et al.*, 2022). At the same time, a rather limited mechanistic understanding of embolism measurements also applies to other methods, such as the flow-centrifuge method (López *et al.*, 2019). While the traditional approach of measuring embolism resistance is strongly based on hydraulic conductivity measurements, potential problems that may affect hydraulic measurements include the ionic effect, wounding response (including resin or latex production), artificial induction of embolism, clogging of pit membranes over time, temporal decline of hydraulic conductivity and embolism propagation that is not only pressure-driven (De Baerdemaeker *et al.*, 2019; Bonetti *et al.*, 2021; Guan *et al.*, 2021). However, embolism resistance depends arguably as much on gas availability as on xylem sap presence, with the gas phase having been largely neglected in earlier discussions. As such, one of the major strengths of pneumatic experiments is that gas in embolized conduits – the specific mechanism of xylem conductivity breakdown – is directly addressed. In this sense, the pneumatic method helps unveil differences in the gas diffusion kinetics inside plants due to anatomical differences, a subject largely unexplored (Pereira *et al.*, 2020b; Trabi *et al.*, 2021; Jansen *et al.*, 2022; Peng *et al.*, 2022).

In conclusion, we found multiple lines of evidence (both from simulations of mechanisms of error and from comparisons among datasets of other studies) supporting the inference that Chen *et al.*'s pneumatic method implementation was deeply flawed and produced invalid results for pneumatically derived embolism vulnerability curves. Thus, being required to put the Chen *et al.* results to the side, we find no basis for experimentalists or plant scientists to doubt the scientific value and utility of embolism resistance measurements obtained via properly conducted pneumatic experiments. Finally, we would like to emphasize that progress in science frequently relies on novel methods to address long-standing questions, and we believe that the pneumatic method for characterizing embolism resistance in the xylem tissue of plants (especially as now augmented by automated measurements that can be made with the Pneumatron apparatus) is one of these that offers cost-effective improvements in measurement speed

and ease of implementation in field settings. We caution that incorrect application of methods could falsely make even well-grounded novel approaches appear faulty and can propagate prejudices about the method. Although strengths, weaknesses and limitations of methods should always be carefully assessed, the extensive and growing literature of such careful assessments supports the use of pneumatic experiments as a solid foundation for advancing our understanding of the gas phase in plant xylem and embolism resistance.

Acknowledgements

US National Science Foundation (NSF) awarded DEB-1754803 to MB and SRS. RVR and RSO are fellows of the National Council for Scientific and Technological Development (CNPq, Brazil). LP and SJ acknowledge funding from the Deutsche Forschungsgemeinschaft (DFG, German Research Foundation, project no. 410768178 and 457287575). MB and RSO were funded by GO-AMAZON FAPESP (2013/50533-5) and FAPESP-UoM (2014/50332-2) to collect the data in the Amazon Forest. MB was also financed in part by the Coordenação de Aperfeiçoamento de Pessoal de Nível Superior – Brasil (CAPES) – Finance Code 001 to collect the data in the Amazon Forest. PRLB acknowledges the UK's National Environment Research Council for its grant (NE/V000071/1).

Author contributions

MB, LP and SRS led the first version of this manuscript. MB and LP derived the statistical analysis. PRLB, SJ, RSO, RVR, SRS, MB and LP led the scientific appointments to derive the analysis presented in the manuscript. All authors contributed to writing the manuscript.

ORCID

Paulo R. L. Bittencourt https://orcid.org/0000-0002-1618-9077
Mauro Brum https://orcid.org/0000-0002-9790-254X
Steven Jansen https://orcid.org/0000-0002-4476-5334
Rafael S. Oliveira https://orcid.org/0000-0002-6392-2526
Luciano Pereira https://orcid.org/0000-0003-2225-2957
Rafael Vasconcelos Ribeiro https://orcid.org/0000-0002-1148-6777
Scott R. Saleska https://orcid.org/0000-0002-4974-3628

Data availability

Data are available in doi: 10.17632/w25bfb8wcz.1.

Mauro Brum[1]*, Luciano Pereira[2], Rafael Vasconcelos Ribeiro[3], Steven Jansen[2], Paulo R. L. Bittencourt[4], Rafael S. Oliveira[5] and Scott R. Saleska[1]*

[1]Department of Ecology and Evolutionary Biology, University of Arizona, Tucson, AZ 85721-0088, USA;
[2]Institute of Systematic Botany and Ecology, Ulm University, Albert-Einstein-Allee 11 89081 Ulm, Germany;
[3]Laboratory of Crop Physiology, Department of Plant Biology, Institute of Biology, University of Campinas (UNICAMP), PO Box 6109, 13083-970 Campinas, SP, Brazil;
[4]College of Life and Environmental Sciences, University of Exeter, Exeter, EX4 4RJ, UK;
[5]Department of Plant Biology, Institute of Biology, UNICAMP, PO Box 6109, 13083-970 Campinas, SP, Brazil
(*Authors for correspondence: email maurobrumjr@gmail.com (MB); saleska@arizona.edu (SRS))

References

Avila RT, Guan X, Kane CN, Cardoso AA, Batz TA, DaMatta FM, Jansen S, McAdam SA. 2022. Xylem embolism spread is largely prevented by interconduit pit membranes until the majority of conduits are gas-filled. *Plant, Cell & Environment* **45**: 1204–1215.

Bonetti S, Breitenstein D, Fatichi S, Domec JC, Or D. 2021. Persistent decay of fresh xylem hydraulic conductivity varies with pressure gradient and marks plant responses to injury. *Plant, Cell & Environment* **44**: 371–386.

Brodersen C, McElrone A. 2013. Maintenance of xylem network transport capacity: a review of embolism repair in vascular plants. *Frontiers in Plant Science* **4**: 108.

Brodribb TJ, Carriqui M, Delzon S, Lucani C. 2017. Optical measurement of stem xylem vulnerability. *Plant Physiology* **174**: 2054–2061.

Brum M, Vadeboncoeur MA, Ivanov V, Asbjornsen H, Saleska S, Alves LF, Penha D, Dias JD, Aragão LE, Barros F *et al.* 2019. Hydrological niche segregation defines forest structure and drought tolerance strategies in a seasonal Amazon forest. *Journal of Ecology* **107**: 318–333.

Chen YJ, Maenpuen P, Zhang YJ, Barai K, Katabuchi M, Gao H, Kaewkamol S, Tao LB, Zhang JL. 2021. Quantifying vulnerability to embolism in tropical trees and lianas using five methods: can discrepancies be explained by xylem structural traits? *New Phytologist* **229**: 805–819.

Choat B, Badel E, Burlett R, Delzon S, Cochard H, Jansen S. 2016. Noninvasive measurement of vulnerability to drought-induced embolism by X-ray microtomography. *Plant Physiology* **170**: 273–282.

Choat B, Brodribb TJ, Brodersen CR, Duursma RA, López R, Medlyn BE. 2018. Triggers of tree mortality under drought. *Nature* **558**: 531–539.

Cochard H, Delzon S, Badel E. 2015. X-ray microtomography (micro-CT): a reference technology for high-resolution quantification of xylem embolism in trees. *Plant, Cell & Environment* **38**: 201–206.

Cook RD. 1979. Influential observations in linear regression. *Journal of the American Statistical Association* **74**: 169–174.

De Baerdemaeker NJ, Arachchige KNR, Zinkernagel J, Van den Bulcke J, Van Acker J, Schenk HJ, Steppe K. 2019. The stability enigma of hydraulic vulnerability curves: addressing the link between hydraulic conductivity and drought-induced embolism. *Tree Physiology* **39**: 1646–1664.

Guan X, Pereira L, McAdam SA, Cao KF, Jansen S. 2021. No gas source, no problem: proximity to pre-existing embolism and segmentation affect embolism spreading in angiosperm xylem by gas diffusion. *Plant, Cell & Environment* **44**: 1329–1345.

Hochberg U, Herrera JC, Cochard H, Badel E. 2016. Short-time xylem relaxation results in reliable quantification of embolism in grapevine petioles and sheds new light on their hydraulic strategy. *Tree Physiology* **36**: 748–755.

Jansen S, Bittencourt P, Pereira L, Schenk HJ, Kunert N. 2022. A crucial phase in plants – it's a gas, gas, gas! *New Phytologist* **233**: 1556–1559.

Jansen S, Guan X, Kaack L, Trabi C, Miranda MT, Ribeiro RV, Pereira L. 2020. The Pneumatron estimates xylem embolism resistance in angiosperms based on gas diffusion kinetics: a mini-review. *Acta Horticulturae* **1300**: 193–200.

Kanduč M, Schneck E, Loche P, Jansen S, Schenk HJ, Netz RR. 2020. Cavitation in lipid bilayers poses a strict negative pressure stability limit in biological liquids. *Proceedings of the National Academy of Sciences, USA* **117**: 10733–10739.

Körner C. 2019. No need for pipes when the well is dry – a comment on hydraulic failure in trees. *Tree Physiology* **39**: 695–700.

López R, Nolf M, Duursma RA, Badel E, Flavel RJ, Cochard H, Choat B. 2019. Mitigating the open vessel artefact in centrifuge-based measurement of embolism resistance. *Tree Physiology* **39**: 143–155.

McDowell N, Pockman WT, Allen CD, Breshears DD, Cobb N, Kolb T, Plaut J, Sperry J, West A, Williams DG *et al.* 2008. Mechanisms of plant survival and mortality during drought: why do some plants survive while others succumb to drought? *New Phytologist* **178**: 719–739.

Meinzer FC, Johnson DM, Lachenbruch B, McCulloh KA, Woodruff DR. 2009. Xylem hydraulic safety margins in woody plants: coordination of stomatal control of xylem tension with hydraulic capacitance. *Functional Ecology* **23**: 922–930.

Paligi SS, Link RM, Isaza E, Bittencourt P, Cabral JS, Jansen S, Oliveira RS, Pereira L, Schuldt B. 2021. Accuracy of the pneumatic method for estimating xylem vulnerability to embolism in temperate diffuse-porous tree species. *bioRxiv*. doi: 10.1101/2021.02.15.431295.

Pammenter NW, Vander Willigen C. 1998. A mathematical and statistical analysis of the curves illustrating the vulnerability of xylem to cavitation. *Tree Physiology* **18**: 589–593.

Peng G, Geng H, Li Y, Ren Z, Peng J, Cao L, Pereira L, Tyree MT, Yang D. 2022. The theory behind vessel length determination using gas flow rates and a comparison between two pneumatic methods based on seven species. *Journal of Experimental Botany* **73**: 5612–5621.

Pereira L, Bittencourt PR, Oliveira RS, Junior MB, Barros FV, Ribeiro RV, Mazzafera P. 2016. Plant pneumatics: stem air flow is related to embolism – new perspectives on methods in plant hydraulics. *New Phytologist* **211**: 357–370.

Pereira L, Bittencourt PR, Pacheco VS, Miranda MT, Zhang Y, Oliveira RS, Groenendijk P, Machado EC, Tyree MT, Jansen S *et al.* 2020a. The Pneumatron: an automated pneumatic apparatus for estimating xylem vulnerability to embolism at high temporal resolution. *Plant, Cell & Environment* **43**: 131–142.

Pereira L, Bittencourt PR, Rowland L, Brum M, Miranda MT, Pacheco VS, Oliveira R, Machado E, Jansen S, Ribeiro RV. 2021. Using the pneumatic method to estimate embolism resistance in species with long vessels: a commentary on the article "A comparison of five methods to assess embolism resistance in trees". *Forest Ecology and Management* **479**: 118547.

Pereira L, Miranda MT, Pires GS, Pacheco VS, Guan X, Kaack L, Karimi Z, Machado EC, Jansen S, Tyree MT *et al.* 2020b. A semi-automated method for measuring xylem vessel length distribution. *Theoretical and Experimental Plant Physiology* **32**: 331–340.

Piñeiro G, Perelman S, Guerschman JP, Paruelo JM. 2008. How to evaluate models: observed vs. predicted or predicted vs. observed? *Ecological Modelling* **216**: 316–322.

R Core Team. 2020. *R: a language and environment for statistical computing*, v.3.5.1. Vienna, Austria: R Foundation for Statistical Computing. [WWW document] URL https://www.R-project.org/

Sergent AS, Varela SA, Barigah TS, Badel E, Cochard H, Dalla-Salda G, Delzon S, Fernandes ME, Guillemot J, Gyenge J *et al.* 2020. A comparison of five methods to assess embolism resistance in trees. *Forest Ecology and Management* **468**: 118175.

Sorz J, Hietz P. 2006. Gas diffusion through wood: implications for oxygen supply. *Trees* **20**: 34–41.

Sperry JS, Hacke UG, Oren R, Comstock JP. 2002. Water deficits and hydraulic limits to leaf water supply. *Plant, Cell & Environment* **25**: 251–263.

Sperry JS, Tyree MT. 1988. Mechanism of water stress-induced xylem embolism. *Plant Physiology* **88**: 581–587.

Trabi CL, Pereira L, Guan X, Miranda MT, Bittencourt PR, Oliveira RS, Ribeiro RR, Jansen S. 2021. A user manual to measure gas diffusion kinetics in plants: pneumatron construction, operation, and data analysis. *Frontiers in Plant Science* **12**: 633595.

Wang Y, Liu J, Tyree MT. 2015. Stem hydraulic conductivity depends on the pressure at which it is measured and how this dependence can be used to assess the tempo of bubble pressurization in recently cavitated vessels. *Plant Physiology* **169**: 2597–2607.

Warton DI, Duursma RA, Falster DS, Taskinen S. 2012. SMATR 3 – an R package for estimation and inference about allometric lines. *Methods in Ecology and Evolution* **3**: 257–259.

Warton DI, Wright IJ, Falster DS, Westoby M. 2006. Bivariate line-fitting methods for allometry. *Biological Reviews* **81**: 259–291.

Wehr R, Saleska SR. 2017. The long-solved problem of the best-fit straight line: application to isotopic mixing lines. *Biogeosciences* **14**: 17–29.

Yang D, Pereira L, Peng G, Ribeiro RV, Kaack L, Jansen S, Tyree MT. 2021. A unit pipe pneumatic model to simulate gas kinetics during measurements of embolism in excised angiosperm xylem. *bioRxiv*. doi: 10.1101/2021.02.09.430450.

Zhang Y, Lamarque LJ, Torres-Ruiz JM, Schuldt B, Karimi Z, Li S, Qin DW, Bittencourt P, Burlett R, Cao KF *et al.* 2018. Testing the plant pneumatic method to estimate xylem embolism resistance in stems of temperate trees. *Tree Physiology* **38**: 1016–1025.

Supporting Information

Additional Supporting Information may be found online in the Supporting Information section at the end of the article.

Fig. S1 Vulnerability curves based on the percentage of air discharge and percentage loss of hydraulic conductance for eight angiosperm species from a seasonal Amazon Forest, FLONA-Tapajós, Pará, Brazil.

Fig. S2 Example of how we calculated the effect of stopping the branch desiccation process early using the pneumatic method in contrast to another method.

Fig. S3 Fraction of the $P_{50.ref}$ induced by the corresponding simulated underestimates of AD_{max} as quantified by the Relative ΨPAD_{max} index, across the eight species and across all simulations, and the $P_{50.simulated}$ as a function of the simulated AD_{max}, showing how they covary in each simulation.

Fig. S4 Cook's distance (calculated for each observation) identifies observations that most strongly influence the statistical model fit between pneumatically-estimated P_{50} and P_{50} determined by a different method, along with the corresponding scatterplot of P_{50} (pneumatic) vs P50 (reference method).

Fig. S5 Reproduction (annotated) of fig. 6 of Chen *et al.* (2021), showing (quoting the caption of Chen *et al.*), 'The kinetics of extracted air volume (ΔVi, μl)' against a broader range of water potentials than used in their standard approach (Fig. 1).

Table S1 Studies that compare P_{50} or P_{88} values from the pneumatic method with other methods.

Table S2 Taxonomic of eight tree species studied at the Tapajos National Forest, km 67 LBA study area, Brazil.

Table S3 Fit using standardized major axis regression.

Please note: Wiley is not responsible for the content or functionality of any Supporting Information supplied by the authors. Any queries (other than missing material) should be directed to the *New Phytologist* Central Office.

Key words: cavitation, drought, phenotyping, tree mortality, water.

Received, 16 February 2022; accepted, 11 August 2022.